Electronic Supplementary Material (ESI) for Nanoscale.

Supporting Information for

Coordination Polymers Derived General Synthesis of Multi-shelled Hollow Metal Oxides for Lithium-ion Batteries

Dongyang Xue,‡[a] Fangfang Xue,‡[a] Xiaoping Lin,[a] Fengyi Zong,[a] Jianmin Zhang[a] and Qiuhong Li*[a]

Pen-Tung Sah Institute of Micro-Nano Science and Technology, Xiamen University, Xiamen 361005, China

E-mail: liqiuhong@xmu.edu.cn; Fax: +86-0592-2187196; Tel: +86-0592-2187198

Experimental details

Synthesis of $ZnCo_2O_4$ and other bimetallic oxides multi-shelled hollow spheres

All chemicals and solvents were of analytical grade and purchased from commercial sources without further purification. In a typical synthesis process, 0.3 mmol $Zn(NO_3)_2 \cdot 6H_2O$, 0.6 mmol $Co(NO_3)_2 \cdot 6H_2O$ and 0.9 mmol p-phthalic acid (PTA) were dissolved in a mixed solvent of DMF (30 mL) and glycerol (15 mL) to form a transparent pink solution by stirring for 2 h. Subsequently, the solution was transferred to a Teflon-lined stainless steel autoclave and kept at 150 ^oC for 6 h. After cooling to room temperature, pink precursor powders were obtained by centrifugation, and washed with ethanol and DMF for several times and dried at 80 ^oC for 24 h in an oven. Then the as-prepared Zn-Co coordination polymer (CPs) were annealed at 500 ^oC for 1 h in air with a heating rate of 1 $^oC\ min^{-1}$ and multi-shelled $ZnCo_2O_4$ hollow spheres were obtained. Other binary microsphere precursors were synthesized by the same method used for Zn-Co CPs and the atomic ratios of Mn/Co, Ni/Co and Ni/Mn were 1:2. During the synthesis process of ZnO-$ZnCo_2O_4$ multi-shelled hollow spheres (MSHSs), the Zn/Co molar ratio was 1:1. Then the multi-shelled hollow binary metal oxides were obtained by the same annealing procedure as that for $ZnCo_2O_4$ hollow spheres.

Synthesis of Co_3O_4 multi-shelled hollow spheres

0.6 mmol $Co(NO_3)_2 \cdot 6H_2O$ and 0.6 mmol p-phthalic acid were dissolved in a mixed solvent of DMF (30 mL) and glycerol (15 mL) to form a transparent pink solution by stirring for 2 h. And then, the solution was transferred to a Teflon-lined

stainless steel autoclave and kept at 150 ^{o}C for 12 h. And the following synthesis steps were similar to those of $ZnCo_2O_4$ multi-shelled hollow spheres.

Synthesis of Mn-Co-Zn, Ni-Co-Mn, Ni-Co-Zn oxides multi-shelled hollow spheres

Using the synthesis process of Mn-Co-Zn oxides as an example, 0.3 mmol $MnCl_2 \cdot 4H_2O$, 0.6 mmol $Co(NO_3)_2 \cdot 6H_2O$, 0.3 mmol $Zn(NO_3)_2 \cdot 6H_2O$ and 1.2 mmol PTA were dissolved in a mixed solvent of DMF (30 mL) and glycerol (15 mL) to form a transparent pink solution by stirring for 2 h. Subsequently, the solution was transferred to a Teflon-lined stainless steel autoclave and kept at 150 ^{o}C for 8 h. The Ni-Co-Zn and Ni-Co-Mn microsphere precursors were obtained through similar procedures of synthesizing Mn-Co-Zn CPs by simply replacing 0.3 mmol Mn^{3+} with 0.3 mmol Ni^{2+}, or 0.3 mmol Zn^{3+} with 0.3 mmol Ni^{2+}, respectively. The multi-shelled hollow ternary metal oxides were generated via a similar thermal treatment of the corresponding precursors.

Materials Characterization

The X-ray diffraction (XRD) patterns of the products were collected by using an X-ray diffractometer (Rigaku Ultima IV) with Cu-K_α radiation at 35 kV and 25 mA in the scanning angle from 10° to 90°. Transmission electron microscopy (TEM; JEOL JEM-2100) and scanning electron microscope (SEM; ZEISS SUPRA 55) were used to characterize the morphology and structure of the samples. The elemental compositions of the samples were investigated by energy dispersive spectroscopy (EDS). Thermo-gravimetric analysis (TGA) was performed on a TG 209 F1 thermal

analyzer at a heating rate of 10 ^{o}C min^{-1} in a temperature range from room temperature to 800 ^{o}C. X-ray photoelectron spectroscopy (XPS, K-Alpha) was conducted to investigate the chemical compositions and element valence state of the samples. Fourier transform infrared spectroscopy (FTIR, Nicolet Avatar 330) was applied to investigate the information of functional group in the samples.

Electrochemical measurements

The electrochemical performance of $ZnCo_2O_4$ and Co_3O_4 MSHSs were investigated by using CR2032 coin cells. The working electrode slurry was prepared by mixing 80 wt% active materials, 10 wt% acetylene black, 10 wt% sodium carboxymethyl cellulose and a certain amount of deionized water. After stirring evenly, the slurry was pasted onto the rough surface of a clean copper foil acting as current collector, followed by drying at 85 ^{o}C in a vacuum oven for 12 h. The mass loading of electrode was about 0.8-1.0 mg cm^{-2}.The fresh coin cells were assembled in a glove box which was filled with argon using lithium foils as reference electrodes and Celgard 2400 as the separator membrane. The electrolyte were composed of 1 M $LiPF_6$ in a compound of ethylene carbonate (EC), diethyl carbonate (DMC) (v/v = 1:1). Galvanostatic charge/discharge cycles were conducted by a battery tester (LAND CT2001A) within a voltage range from 0.01 to 3.00 V. A CHI 660E electrochemical workstation (Shanghai Chenhua Instrument Co., China) was applied to test the cyclic voltammogram (CV) at a scanning rate of 0.1 mVs^{-1}.

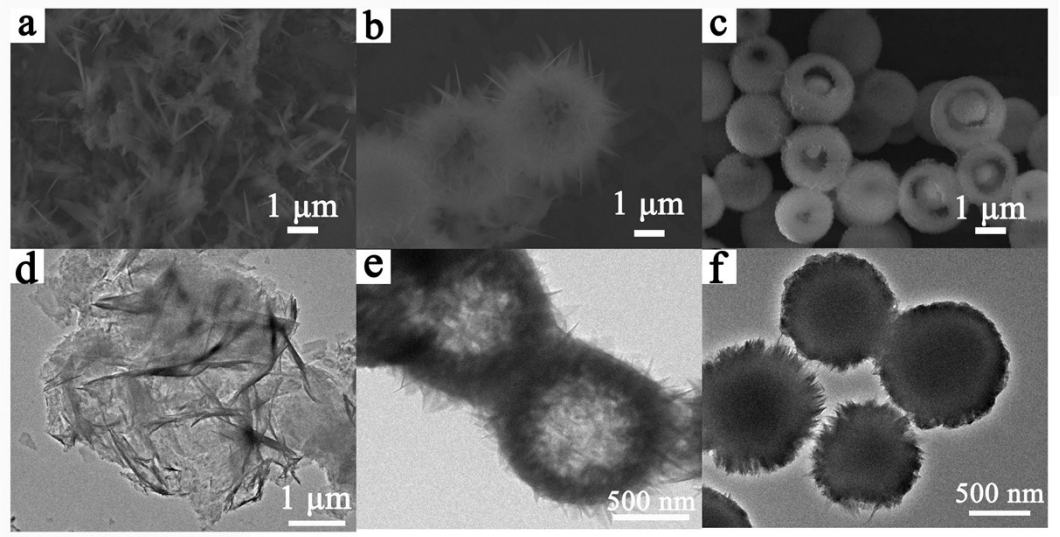

Figure S1. (a-c) SEM images and (d-f) TEM images of the precursors collected after (a, d) 0.5, (b, e) 1 and (c, f) 6 h of reaction.

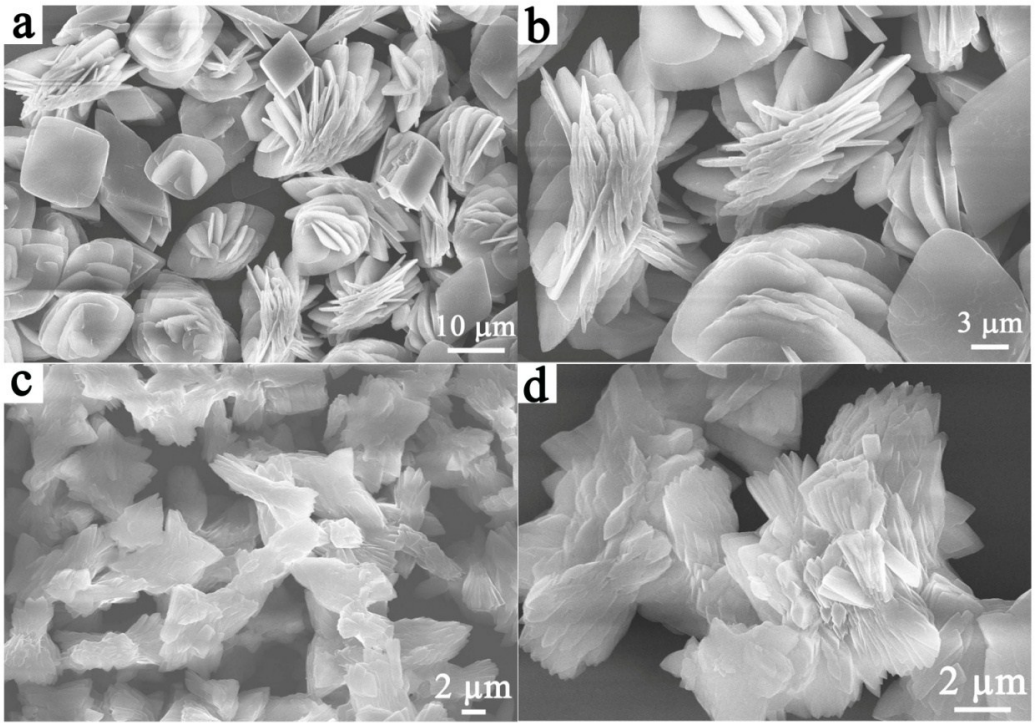

Figure S2. SEM images of the products prepared without PTA (a-b) or glycerol (c-d).

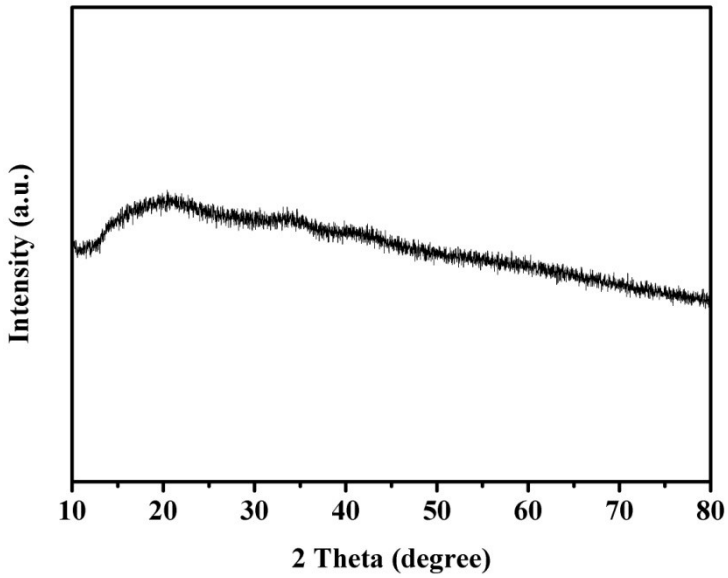

Figure S3. XRD pattern of Zn-Co CPs.

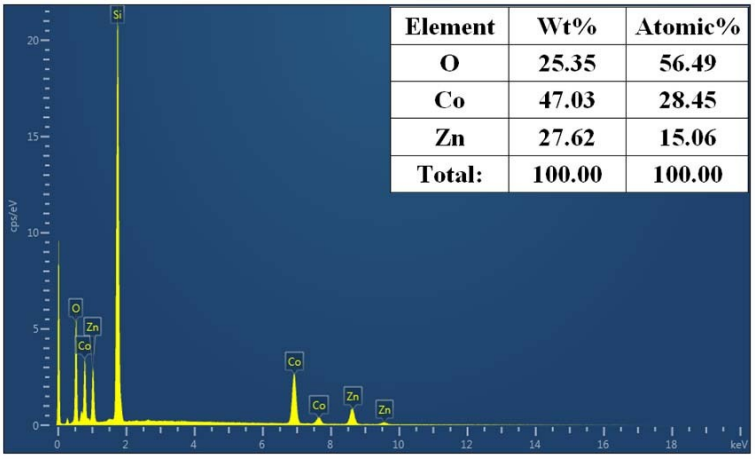

Element	Wt%	Atomic%
O	25.35	56.49
Co	47.03	28.45
Zn	27.62	15.06
Total:	100.00	100.00

Figure S4. EDS spectrum of $ZnCo_2O_4$ MSHSs.

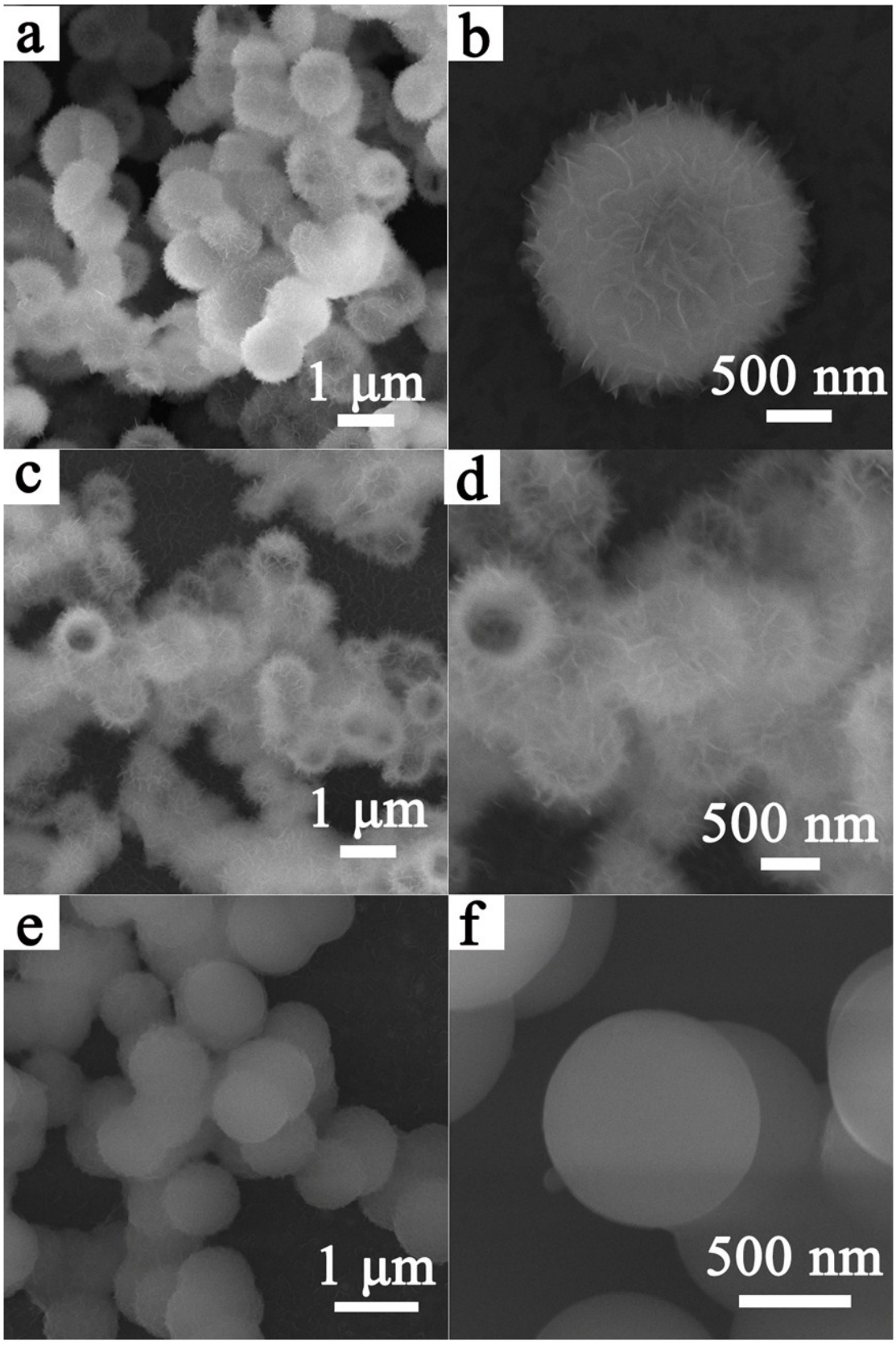

Figure S5. SEM images of (a-b) Mn-Co CPs, (c-d) Ni-Co CPs, and (e-f) Ni-Mn CPs at different magnifications.

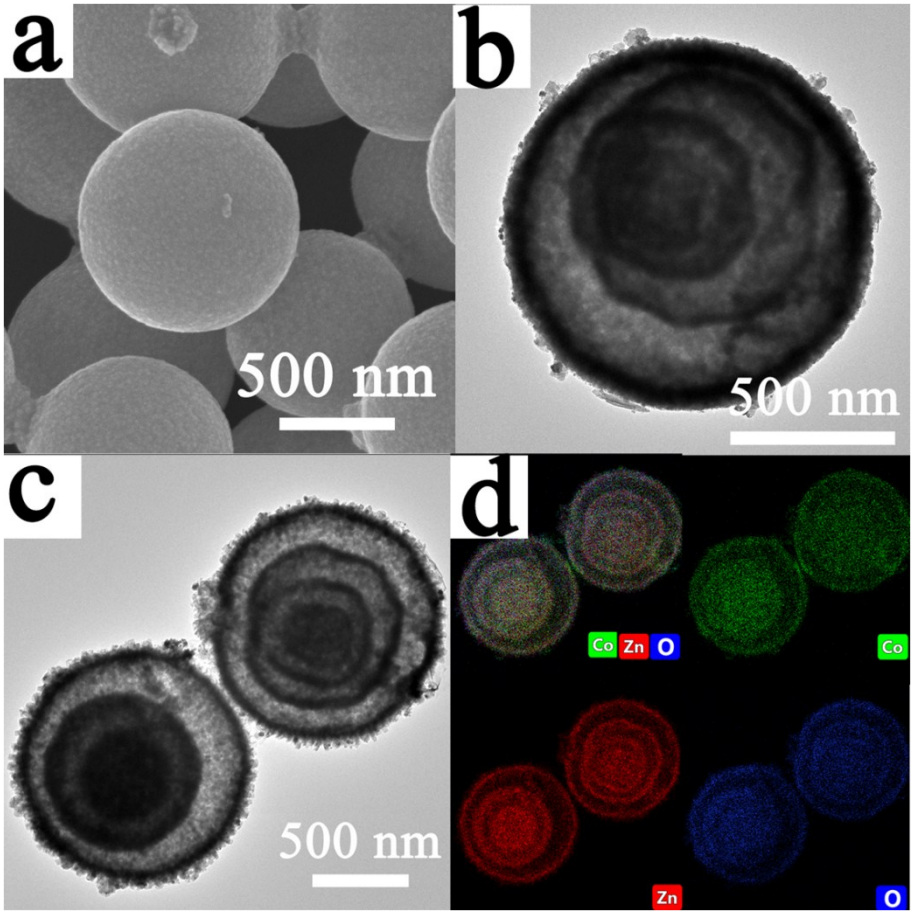

Figure S6. (a) SEM image and (b-c) TEM images of ZnO- $ZnCo_2O_4$ MSHSs, (d) EDS mapping images of ZnO-$ZnCo_2O_4$ MSHSs.

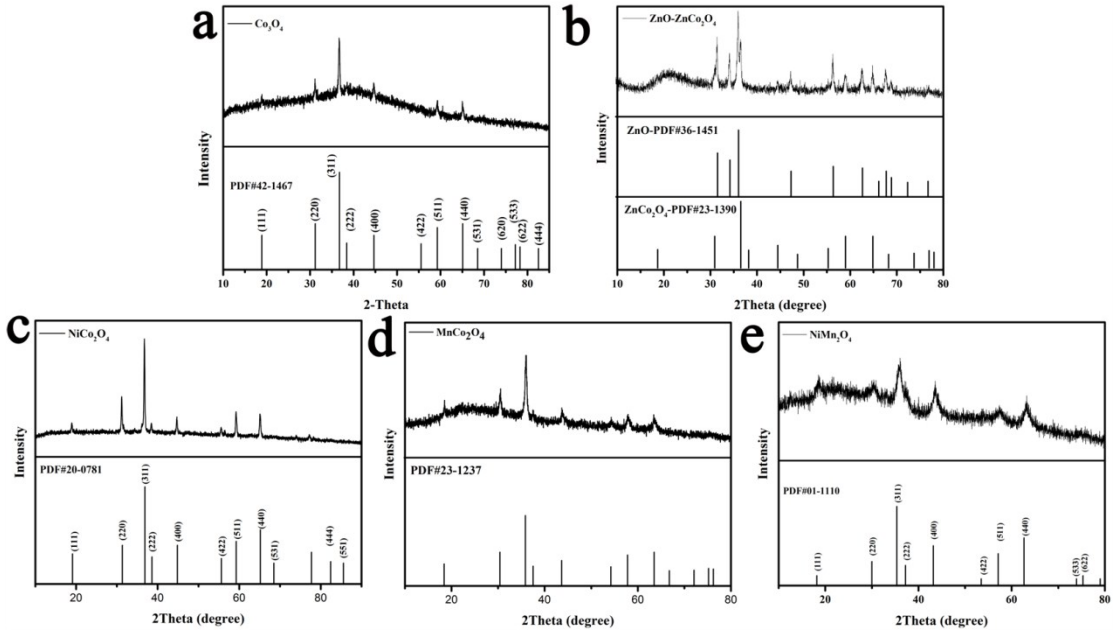

Figure S7. XRD patterns of as-prepared (a) Co_3O_4, (b) ZnO-$ZnCo_2O_4$, (c) $NiCo_2O_4$, (d) $MnCo_2O_4$, and (e) $NiMn_2O_4$.

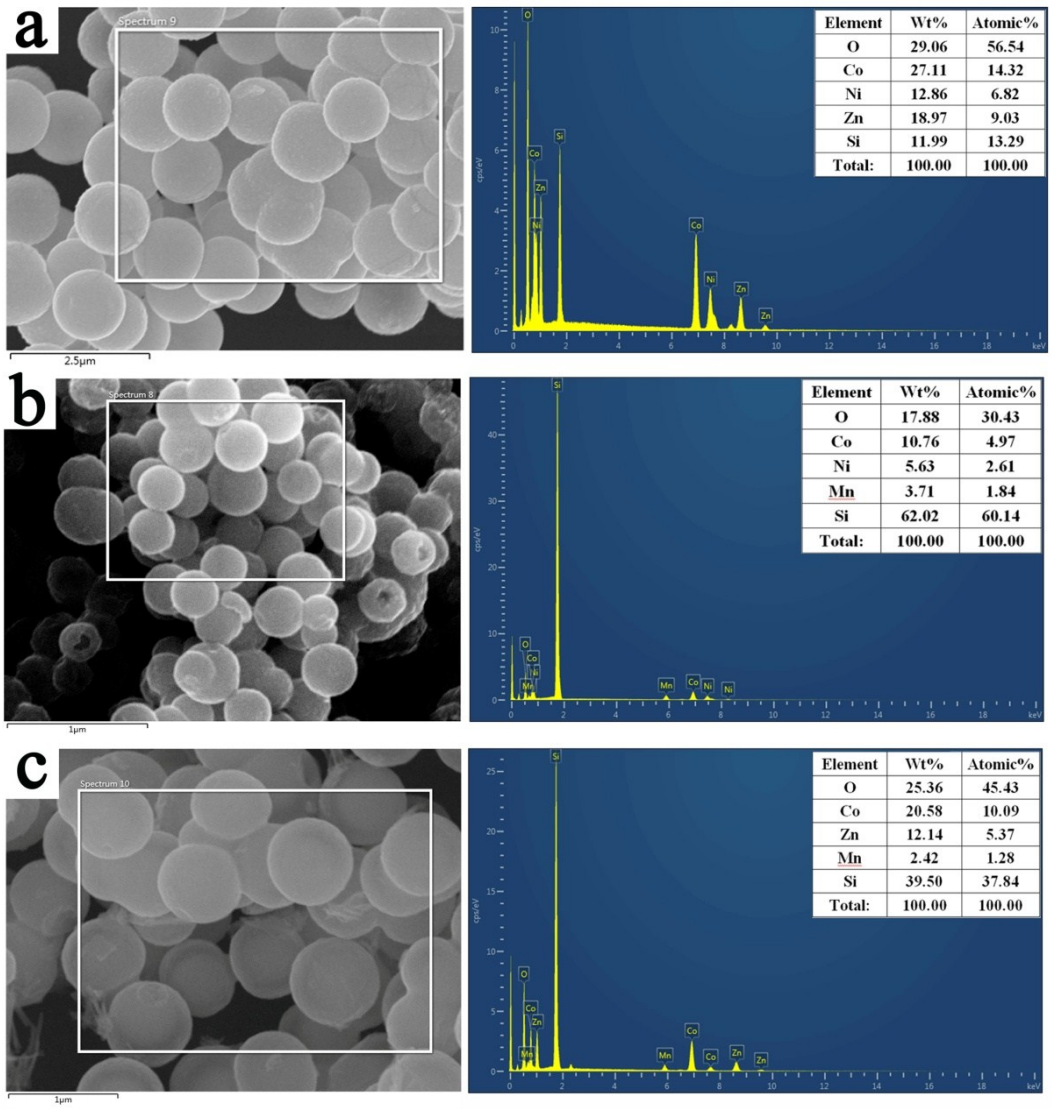

Figure S8. EDS results of (a) Ni-Co-Zn oxides, (b) Ni-Co-Mn oxides, and (c) Mn-Co-Zn oxides.

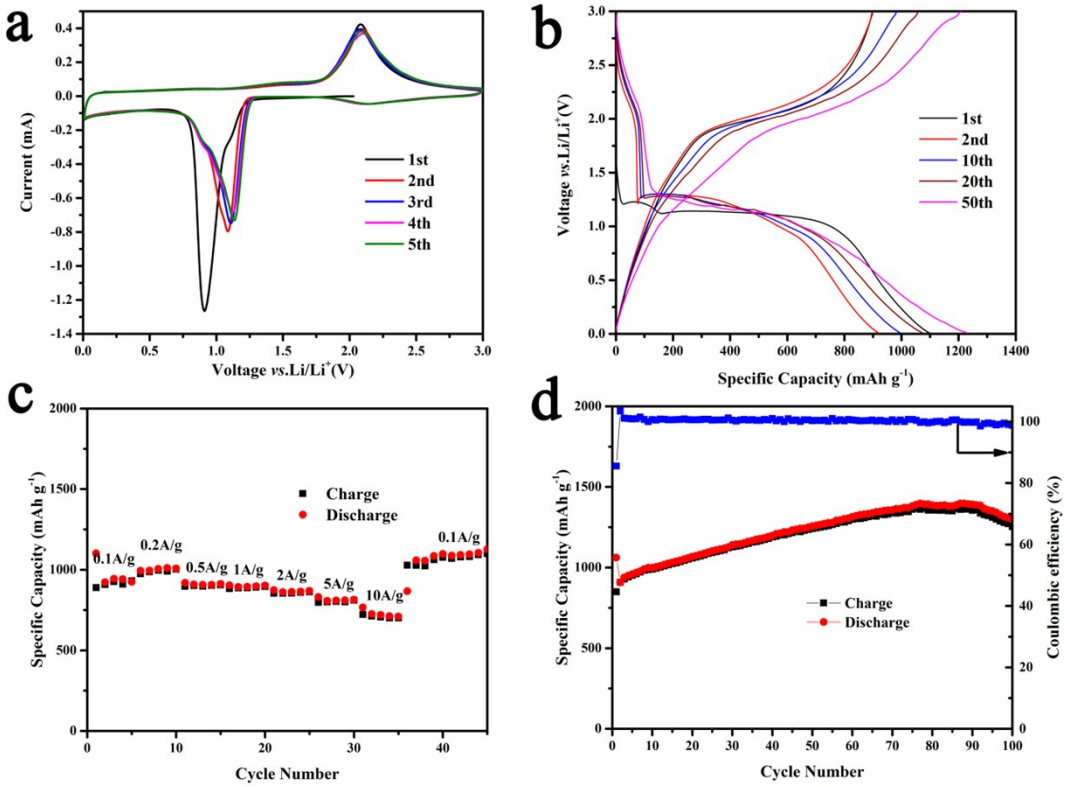

Figure S9. (a) CV curves of Co_3O_4 MSHSs at a scan rate of 0.1 mV s^{-1} in a potential range from 0.01 to 3.0 V; (b) charge-discharge curves of Co_3O_4 MSHSs at a current density of 100 mA g^{-1}; (c) rate performance of Co_3O_4 MSHSs; (d) cycling performance of Co_3O_4 MSHSs at a current density of 500 mA g^{-1}.

Figure S9a illustrates the first five CV curves of Co_3O_4 MSHSs anode in a voltage range from 0.01 to 3.0 V at a scanning rate of 0.1 mV s^{-1}. In the first cathodic scan, a distinct reduction peak located at 0.91 V is ascribed to the decomposition of Co_3O_4 to metallic Co and the transition of Li to amorphous Li_2O together with the formation of SEI film[1]. In the first anodic scan, a distinct oxidation peak at 2.08 V corresponds to the oxidation of metallic Co to Co^{3+} accompanied with the decomposition of Li_2O to form lithium. In the subsequent cycles, the reduction peaks shift to 1.1 V together with sharply decreased intensity, indicating a different

electrochemical mechanisms from the first anodic process. Typical galvanostatic charge/discharge curves of Co_3O_4 MSHSs anode at 100 mA g^{-1} are shown in Figure S9b. The discharge/charge curves of 2^{nd}, 10^{th}, 20^{th}, 50^{th} shift to the right gradually, indicating that the specific capacity of Co_3O_4 MSHSs electrode increases gradually during the following lithium-storage process. The rate capabilities of Co_3O_4 MSHSs anode is investigated under different current densities ranging from 0.1 to 10 A g^{-1} (Figure S9c). The Co_3O_4 MSHSs electrode exhibits high reversible capacities of 944, 1010, 906, 897, 869, 813, 720 mAh·g^{-1} at current densities of 0.1, 0.2, 0.5, 1.0, 2.0, and 5.0 A g^{-1} respectively. Noticeably, when the current density is returned to 0.1 A g^{-1}, the specific capacity is reversibly back to 1100 mAh·g^{-1} after 10 cycles. The results suggests that Co_3O_4 MSHSs maintain extraordinary structural stability even under high current density. Obviously, the discharge capacity (1010 mAh·g^{-1}) at 0.2 A g^{-1} is even higher than that at 0.1 A g^{-1}, which is probably caused by the gradual active process of multi-shell structures and transition metal oxides[2]. Furthermore, the Co_3O_4 MSHSs electrode shows excellent cyclic stability at a current density of 500 mA g^{-1}. Apparently, the capacity of Co_3O_4 MSHSs increases from initial 849 to 1380 mAh·g^{-1} and still retains the capacity of 1300 mAh·g^{-1} after 100 cycles. This results illustrated that Co_3O_4 MSHSs possess similar superior electrochemical performance as $ZnCo_2O_4$ MSHSs.

Table S1 Electrochemical performance of different Zn-Co based electrodes.

Type of materials	Cycling performance	Rate capability	Ref.
rGO/$ZnCo_2O_4$ nanocomposite	960.8 mA h g^{-1} after 100 cycles at 90 mA g^{-1}	593.2 mA h g^{-1} at 900 mA g^{-1}	[3]
$ZnCo_2O_4$ nanoparticles	770 mAh g^{-1} after 50 cycles at 60 mA g^{-1}	~430 mAh g^{-1} at 240 mA g^{-1}	[4]
$ZnCo_2O_4$ yolk-shelled microspheres	331 mA h g^{-1} after 500 cycles at 1000 mA g^{-1}	553 mA h g^{-1} at 2000 mA g^{-1}	[5]
Double-shelled $ZnCo_2O_4$ hollow microspheres	1019 mAh g^{-1} after 120 cycles at 90 mA g^{-1}	570 mA h g^{-1} at 4500 mA g^{-1}	[6]
Mesoporous $ZnCo_2O_4$ microsphere	721 mAh g^{-1} after 80 cycles at 0.1 A g^{-1}	435 mA h g^{-1} at 2 A g^{-1}	[7]
Multi-shelled hollow $ZnCo_2O_4$ sphere	1300 mA h g^{-1} after 200 cycles at 100 mA g^{-1}	450 mA h g^{-1} at 10 A g^{-1}	This work

References

[1] Y. G. Li, B. Tan and Y. Y. Wu, Nano Letters, 2008, 8, 265-270.

[2] J. Bai , X. G. Li , G. Z. Liu , Y. T. Qian , and S. L. Xiong, Adv. Funct. Mater. 2014, 24, 3012–3020

[3] G. X. Gao , H. B. Wu , B. T. Dong , S. J. Ding , and X. W. (David) Lou, *Adv. Sci.*,2015, **2**, 1400014.

[4] D. Deng and J. Y. Lee, *Nanotechnology*, 2011,**22**, 355401.

[5] J. F. Li, J. Z. Wang, D. Wexler, D. Q. Shi, J. W. Liang, H. K. Liu, S. L. Xiong and Y. T. Qian, *J. Mater. Chem. A*, 2013, **1**, 15292–15299.

[6] Q. S. Xie, F. Li, H. Z. Guo, L. S. Wang, Y. Z. Chen, G. H. Yue, and D. L. Peng, *ACS Appl. Mater. Interfaces*, 2013, **5**, 5508-5517.

[7] L. L. Hu, B. H. Qu, C. C. Li, Y. J. Chen, L. Mei, D. N. Lei, L. B. Chen, Q. H. Li and T. H. Wang, *J. Mater. Chem. A*, 2013, **1**, 5596–5602.